ARTICLE

Photodissociation Dynamics of Methanol and Ethanol at 157 nm

Kai-jun Yuan, Yuan Cheng, Feng-yan Wang, Xue-ming Yang*

State Key Laboratory of Molecular Reaction Dynamics, Dalian Institute of Chemical Physics, Chinese Academy of Sciences, Dalian 116023, China

(Dated: Received on May 22, 2008; Accepted on June 20, 2008)

157 nm photodissociation of jet-cooled CH_3OH and C_2H_5OH was studied using the high-n Rydberg atom time-of-flight (TOF) technique. TOF spectra of nascent H atom products were measured. Simulation of these spectra reveals three different atomic H loss processes: one from hydroxyl H elimination, one from methyl (ethyl) H elimination, and one from secondary dissociation of the methoxy (ethoxy) radical. The relative branching ratio indicates secondary dissociation of ethoxy is less important than that of methoxy. The average angular anisotropy parameter of methanol is negative (with $\beta\approx-0.3$), indicating the transition dipole moment is perpendicular to the C−O−H plane. The slightly more negative β value of ethanol (with $\beta\approx-0.4$) implies that ethanol has a longer rotational period. These experimental results indicate that both systems undergo fast internal conversion to the 3s surface after it is excited to the $3p_x$ surface, and then dissociate on the 3s surface. The translational energy distribution of the CH_3O+H products reveals extensive CH_3 rocking or CH_3 umbrella excitation in the CH_3O radical. However the vibrational structures are not resolved in the C_2H_5O radical.

Key words: Photodissociation dynamics, H atom channel, VUV photolysis

I. INTRODUCTION

The photochemistry of saturated alcohols has received considerable attention over the last two decades [1,2]. With an alkyl group replacing a hydrogen atom in water, saturated alcohols exhibit spectral features similar to, but distinct from, those of water. Despite numerous experimental and theoretical investigations, the photoexcitation of methanol and ethanol, which are the simplest alcohols, are still poorly understood.

The absorption spectrum of methanol in the region of 105-200 nm (Fig.1) has been reported by Nee *et al.* who have assigned several features of the spectrum [3]. The long wavelength end of the spectrum shows an absorption continuum 165-198 nm that has been assigned to the 3s←n Rydberg transition. Features in the 151-163 and 140-151 nm have been assigned to the different components of the 3p←n Rydberg transitions. Although features in the 140-163 nm regions are associated with 3p-type Rydberg orbitals, they show disparate vibrational structures. Peaks in the 151-163 nm region have irregular spacing ∼800 cm^{-1}, whereas those in the 140-151 nm region show a regular vibrational spacing ∼1000 cm^{-1}. Both progressions were assigned to be associated with the C−O stretching mode. Sominska *et al.* recorded absorption spectra of CH_3OH, CH_3OD, and CD_3OD in a supersonic jet and assigned another vibrational mode (CH_3 rocking) for the system in the region of 151-163 nm [4]. For wavelengths smaller than 140 nm, weak features are superimposed on a rising continuum. Nee *et al.* associated these features with transitions to higher Rydberg states [3].

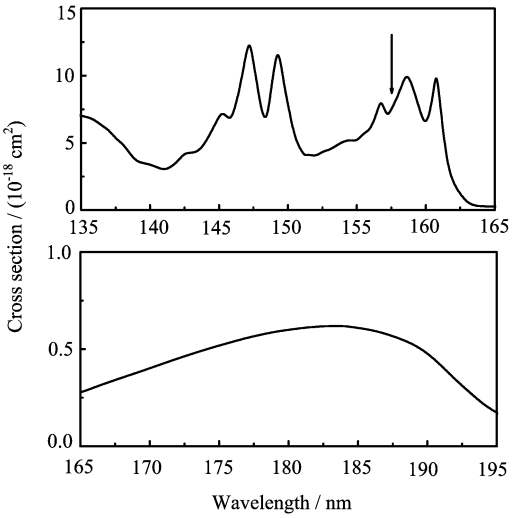

FIG. 1 The UV absorption spectrum of methanol taken from Ref.[3]. The lower panel shows the absorption spectrum in the 165-198 nm region. The broad continuum in this panel is attributed to the 3s←n transition. The upper panel shows the absorption spectrum in the 135-165 nm region. The spectral features have been assigned to the 3p←n transitions. The photolysis wavelength (157 nm) in this work is indicated by the arrow.

In infrared multiple photon dissociation studies [5], it was found that the dominant primary products were the same as those seen in thermal excitation, namely, CH_3+OH. Recently, Satyapal *et al.* studied photolysis of methanol at 193.3 nm by using laser-induced fluorescence (LIF) spectra of nascent H-atom prod-

*Author to whom correspondence should be addressed. E-mail: xmyang@dicp.ac.cn

ucts [6]. However, they found that O−H bond fission is the dominant channel, with a quantum yield of 0.86±0.10. They also measured the translational energy release ($\langle E_T \rangle$=0.82 E_{avail}) and the angular distribution (β=−0.6) of the CH_3O+H channel. *Ab initio* calculations [7-9] show that the first excited state (3s Rydberg state) of methanol is purely repulsive in the OH coordinate, thus the dissociation of the hydroxyl H is most likely from direct dissociation on the repulsive 3s surface. The C−O bond is also repulsive, but there is a small barrier to dissociation that hinders propagation through this channel. Wen *et al.* studied photodissociation of methanol at 193.3 nm using the high-n Rydberg atom time-of-flight (HRTOF) technique, and confirmed that O−H bond dissociation is the main source of H-atom products [10]. Furthermore, they obtained a vibrationally resolved internal energy distribution of methoxy from translational energy spectra, revealing a methoxy C−O stretching progression that peaks at v=1 and extends to v=5.

Photodissociation of methanol on the second excited state (3p Rydberg state) is more complicated. Harich *et al.* obtained photofragment time-of-flight (TOF) spectra at m/e=1(H), 2(H_2,D), 3(HD), and 4(D_2) for CH_3OH, CH_3OD, and CD_3OH at 157 nm excitation using universal crossed molecular beam apparatus [11,12]. Analysis of those experimental results revealed three different atomic H loss processes: one type of direct hydroxyl H elimination and two types of methyl H elimination. Lee *et al.* investigated distributions of angular anisotropy parameter and translational energy of fragments for photolysis of methanol at 157 nm using TOF mass spectrometry [13,14]. They found that the average β value of hydroxyl H is −0.26, while the β value of methyl H is zero. They suggested that the transition dipole moment is almost perpendicular to the C−O−H plane and that n-$3p_x$ is the major photoexcited state at 157 nm.

Photochemical studies of ethanol, the next larger saturated alcohol, are limited. End product studies imply that, similar to methanol, ethanol O−H bond fission is the major dissociation channel [2,7,15]. The first absorption band of ethanol at ∼180 nm is associated with that of H_2O and has been assigned to an n_O-σ^* transition. This electronic excitation is localized (primarily on the H−O−C moiety), as in a case of methanol. It is anticipated that photochemistry of ethanol should be similar to that of methanol. Satyapal *et al.* investigated the H-atom channel in 193.3 nm photolysis of ethanol by using H-atom LIF spectra [6]. They measured the translational energy release ($\langle E_T \rangle$=0.71 E_{avail}) of the C_2H_5O+H channel. Xu *et al.* also studied photodissociation of jet-cooled C_2H_5OH and C_2H_5OD at 193.3 nm using HRTOF technique [16]. They found that the H-atom photofragment was produced preferentially from O−H bond fission. They also observed extensive C−O stretch and modest C−C−O bending excitation in the C_2H_5O radical, which could be rationalized by the geometric change in going from the parent molecule to the excited surface and then to the ethoxy radical product. The H atom product angular distribution was anisotropic (with β=−0.9), indicating a perpendicular electronic transition and a short excited state lifetime.

In this study, photodissociation dynamics of methanol and ethanol at 157 nm was investigated. TOF spectra of the nascent H atom photofragments were measured using HRTOF technique. Center-of-mass translational energy distributions were derived from the TOF spectra. Polarized radiation was also utilized to obtain H atom product angular distribution.

II. EXPERIMENTS

The high-n Rydberg atom time-of-flight (HRTOF) technique utilized in this study has been described in detail elsewhere [17,18] and only a brief description is presented here. A skimmed molecular beam of CH_3OH (C_2H_5OH), seeded in helium (mixing ratio ∼2.5%, total pressure ∼101 kPa), is crossed at 90° with the output of the photolysis laser (157 nm power 2-4 mJ, with the beam diameter ∼10 mm), which was produced by a Lambda Physik LPX210I F_2 laser. The 157 nm radiation was polarized by a special 157 nm polarizer and focused by an MgF_2 lens. H atom products were tagged by excitation to high-n Rydberg levels using a two-step excitation scheme: the 121.6 nm excitation to the n=2 level from the groud state and the subsequent 366 nm excitation to a high-n (n=30-80) Rydberg level from the n=2 state. Photons at 121.6 nm are generated by four-wave mixing of two 212.5 nm photons and one 845 nm photon in a cell filled with a 3:1 ratio Ar-Kr mixture. Photons at 212.5 nm are produced by doubling the output of a Nd:YAG (Spectra Physics Pro-290) 3rd harmonic pumped dye laser (Sirah, PESC-G-24) operating at ∼425 nm. A portion of the 532 nm output of the YAG is used to pump another dye laser (Continuum ND6000) operating at ∼845 nm. These beams are then focused into a mixing cell where four-wave mixing at 121.6 nm is generated. The remainder of the 532 nm source is used to pump a third dye laser (Radiant Dye Laser-Jaguar, D90MA), operating at ∼732 nm, the output from which frequence is doubled to ∼366 nm, and used to promote the H atoms from the n=2 level to a high-n Rydberg state, lying just below the ionization threshold. Ions formed at the tagging region by initial laser excitation are extracted away from the TOF axis by a small electric field (∼30 V/cm) placed across the interaction region.

The tagged H atoms then fly a certain TOF distance (∼333 mm) to reach a MCP detector with a fine metal grid (grounded) in the front. After passing through the grid, the Rydberg atoms are then immediately field-ionized by the electric field applied between the front plate of the Z-stack MCP detector and the fine metal grid. The signal detected by the MCP is then amplified

DOI:10.1088/1674-0068/21/04/301-307

by a fast pre-amplifier, and counted by a multichannel scaler.

About 2.6 kPa CH_3OH (C_2H_5OH) was stored in the stainless steel container and He gas was immediately filled to produce 2.5% CH_3OH (C_2H_5OH)/He ratio. CH_3OH (99.9%) and C_2H_5OH (99.9%) were purchased from Aldrich. Both compounds were used without purification.

III. RESULTS

A. Photodissociation channels

The energy level diagram of CH_3OH and energetically possible dissociation channels at 157 nm are shown in Fig.2. H atom product channels are the main interest in this study. Figure 3(a) shows the H atom product TOF spectrum for photodissociation of CH_3OH. There are two distinctive features in this spectrum, one fast and sharp peak with some vibrational structures, and one slow and broad peak. This is indicating that the H atom products come from at least two different dissociation channels. The similar spectrum has been obtained by Harich *et al.* using electron impact ionization technique [12]. Due to low translational energy resolution in their experiments, the vibrational structures have not been observed. It is clear that detection of the H atom by Rydberg tagging technique is more sensitive. The vibrational structures, which will be discussed later, corresponds to the CH_3 rocking. This is indicative of direct dissociation on an excited electronic state surface that correlates with ground state products.

The fast H atom product is clearly from the hydroxyl group of CH_3OH (process (a) in Fig.2), since the earliest H atom TOF signal for process (a) is ∼13.5 μs, which is shown by the downward pointing arrow (in Fig.4(a)), consistently with the onset of the fast peak. The translational energy distribution, P(E)(1) in Fig.5(a), was used to fit the observed TOF peak as a primary two-body process of H+CH_3O. The simulated TOF spectrum for this process is also shown in Fig.4(a) and compared with the experimental data. The high energy cutoff of the translational energy distribution obtained is consistent with the available energy for hydroxyl H loss of CH_3OH. The translational energy distribution is

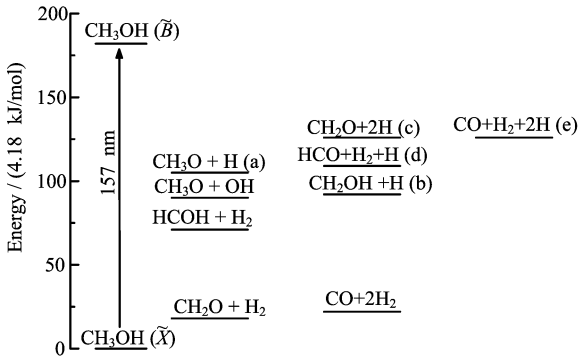

FIG. 2 Energy level diagram of methanol and energetically possible dissociation channels in this experiment. The available energy for a given channel is the difference in height between the photon energy and the channel enthalpy. See Ref.[12] for more details.

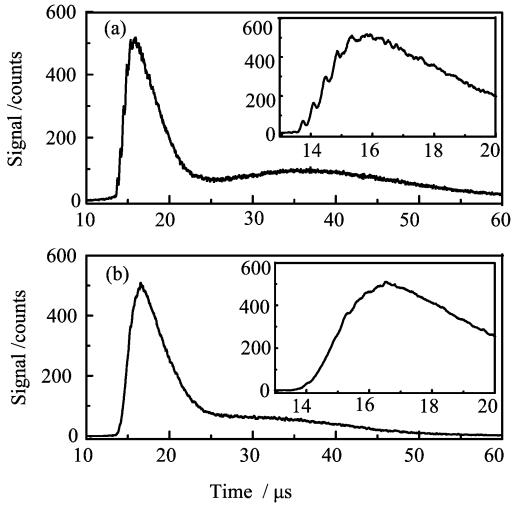

FIG. 3 H-atom TOF spectra for photodissociation of (a) CH_3OH and (b) C_2H_5OH at 157 nm. These spectra were taken by averaging signals over 50 k laser shots. The laser power was 3-5 mJ/pulse.

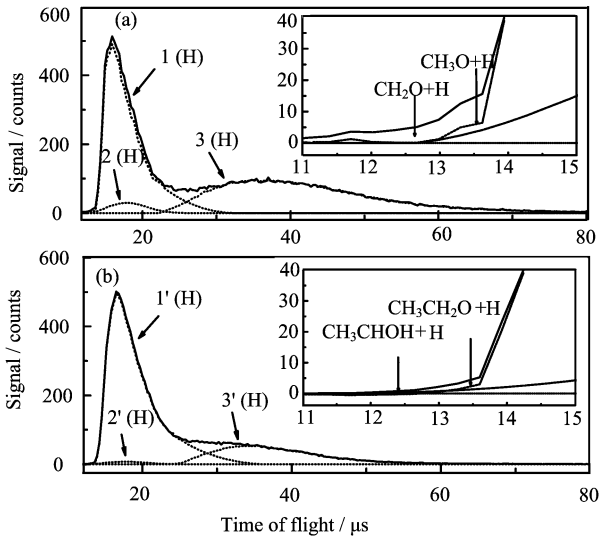

FIG. 4 H-atom TOF spectra for photodissociation of (a) CH_3OH and (b) C_2H_5OH at 157 nm. The dotted curves fit to the spectra represent signals from different processes and were simulated as two-body dissociation of hydroxyl H(1), two-body dissociation of methyl (ethyl) H(2), and secondary (three-body) dissociation of methyl (ethyl) H(3) from the methoxy (ethoxy) radical produced in channel 1. The onsets of H-atom TOF signals in different channels are shown by the downward pointing arrows.

DOI:10.1088/1674-0068/21/04/301-307

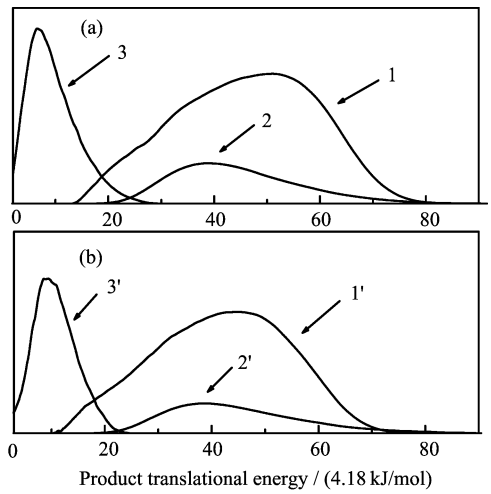

FIG. 5 Translational energy distributions used to simulate the various atomic H atom processes. (a) The distributions for the hydroxyl H loss (1), the two-body methyl H loss (2), and the secondary methoxy H loss (3) from CH_3OH. (b). The distributions for the hydroxyl H loss (1′), the two-body ethyl H loss (2′), and the secondary ethoxy H loss (3′) from C_2H_5OH.

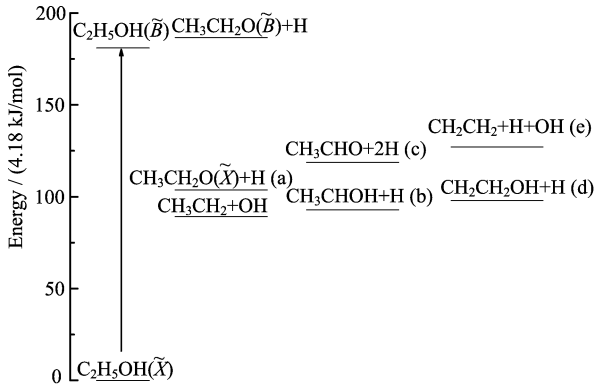

FIG. 6 Energy level diagram of ethanol and energetically possible dissociation channels in this experiment. The available energy for a given channel is the difference in height between the photon energy and the channel enthalpy. Since the H-atom product channels are the main interest in this study, the H_2 product channels are not shown here.

peaked at quite high energy, indicating that a significant amount of the available energy is partitioned into the kinetic energy of the photofragments.

The low-intensity H atom signal with arrival time earlier than 13.5 μs was also observed in Fig.4(a). This implies that other channels might also make some small contribution to the fast feature. The onset of H-atom TOF signal in process (b) (Fig.2) is ∼12.6 μs, which is also shown by the downward pointing arrow (in Fig.4(a)). Therefore, it is not difficult to draw the conclusion that this small fast signal is likely due to the primary H atom elimination from the methyl group in CH_3OH. This dissociation channel has also been observed in the photolysis of CH_3OD by Harich *et al.* [12]. The translational energy distribution, P(E)(2) in Fig.5(a), was used to fit the fast feature as a two-body process of $H+CH_2OH$. The peak for the translational energy distribution P(E)(2) is shifted to low energy, indicating that the dynamical picture of process (b) is much different from that of process (a) (Fig.2). The slower broad feature in Fig.3(a) exhibits a very low product translational energy release (peaked at ∼33.4 kJ/mol). These slow H atom products are probably coming from the CH_3 group. However, the dynamical sources of these slow H atom products are not immediately clear. Due to the fact that the CH_3O radical is unstable and that a CH_3O fragment with internal energy greater than 104.5 kJ/mol dissociates to CH_2O+H, the process (c) in Fig.2 is clearly a possible source for the slow feature. A reasonable fit has been obtained for this slow feature in the TOF spectrum using P(E)(1) (Fig.5(a)) as the translational energy distribution of the primary process $CH_3OH \rightarrow (CH_3O)^* + H$, and P(E)(3) (Fig.5(a)) as the translational energy distribution of the secondary dissociation $(CH_3O)^* \rightarrow H_2CO+H$.

From the above investigations combining with previous experimental results [12], it is quite clear that three types of H atom elimination processes have been identified. The relative intensities of the atomic processes can be calculated from the simulation, which gives the following branching ratio for the atomic H loss processes from CH_3OH: hydroxyl H(1)/methyl H(2)/methoxy H(3)=1:0.07:0.95.

The H-atom TOF spectrum for photodissociation of C_2H_5OH at 157 nm has also been obtained, as shown in Fig.3(b). The spectrum is composed of two distinctive features, one strong and sharp peak, and one small and broad peak, similarly to that for CH_3OH. However, no vibrational structures were observed. To identify the main source of the H-atom product, we draw out the energy level diagram of C_2H_5OH with possible dissociation channels, as shown in Fig.6. The strong and sharp fast H-atom signal is clearly from the hydroxyl group of C_2H_5OH, which is very much similar to the ethanol photodissociation at 193.3 nm excitation. The onset of the fast strong feature is in rather good agreement with the earliest arrival time (∼13.4 μs) for process (a) (Fig.6). The low-intensity H atom signals with arrival time earlier than 13.4 μs were also observed in Fig.4(b). The onsets of H-atom TOF signals for process (b) and (d) (Fig.6) are ∼12.4 and 12.8 μs, respectively. Therefore, these two processes should make some contribution to the low-intensity fast H-atom signal. The broad slow feature in Fig.3(b) exhibits a very low product translational energy release (peaked at ∼37.6 kJ/mol). These slow H atom products are probably coming from the C_2H_5 group. A theoretical estimate found a barrier of ∼87.8 kJ/mol for unimolecular decomposition of ethoxy radical into CH_3CHO+H [19]. Thus, it is clear that process (c) (Fig.6) is the possible source for the slow

DOI:10.1088/1674-0068/21/04/301-307

ethyl H atom elimination. A reasonable fit has been obtained in the spectrum shown in Fig.4(b), similarly to that for CH_3OH. The translational energy distributions, P(E) (1′), (2′), (3′) in Fig.5(b), were used to fit the observed TOF peaks as two-body process (a), two-body process (b) or (d), and three-body process (c) (Fig.6), respectively. The relative intensities of the atomic processes can also be calculated from this simulation. The branching ratio for the atomic H loss processes from C_2H_5OH is determined to be Hydroxy H(1′)/ethyl H (2′)/ethoxy H(3′)=1:0.02:0.30. It is clear that the secondary H elimination of ethoxy is less important than that of methoxy.

B. H-atom product angular distribution

Linearly polarized radiation was also used as the photolysis source to study the H-atom product angular distribution in CH_3OH and C_2H_5OH dissociation. Linearly polarized light preferentially excites the molecules with their electronic transition dipole moment parallel to the electric vector **E** of the polarized laser radiation. The photofragment angular distribution is given by [20]:

$$I(\theta) = \frac{\pi}{4}[1 + \beta P_2(\cos\theta)] \quad (1)$$

where β is the anisotropy parameter ($-1 \leq \beta \leq 2$), θ is the angle between the electric vector **E** and the recoiling velocity vector of the H atom product (the direction of detection), and $P_2(\cos\theta)$ is the second Lengedre polynomial. Figure 7(a) shows the translational energy dependent product anisotropy parameter obtained for CH_3OH photodissociation. It is obvious that the β parameter changes dramatically as a function of the total translational energy. Between the translational energy range of 167-260 kJ/mol, the anisotropy parameter is ~ -0.3, similarly to the reported values for CH_3O+H ($\beta = -0.26$) [14]. Between the translational energy range of 0-125 kJ/mol, the anisotropy parameter is monotonously changing from -0.2 to 0.2. This is indicating that these H atom products do not arise from primary H loss process since the methyl H has an isotropic angular distribution. Thus these H atoms likely come from the secondary dissociation process. While in the translational energy range of 260-313 kJ/mol, the anisotropy parameter is changing from -0.3 to -0.6 with some oscillation. It is obvious that the dynamics for this region is complicated and surface coupling plays an important role. Figure 7(b) shows the translational energy dependent product anisotropy parameter obtained for C_2H_5OH photodissociation. It is obvious that the anisotropy parameter for C_2H_5OH is similar to that for CH_3OH. Between the translational energy range of 0-125 kJ/mol, the anisotropy parameter is weakly dependent on the translational energy. This is quite reasonable since the secondary dissociation for C_2H_5OH is less important than that for CH_3OH. Between the translational energy range of 125-313 kJ/mol, the anisotropy parameter is ~ -0.4, indicating that the hydroxyl H for C_2H_5OH is more anisotropic than that for CH_3OH. The slightly more negative β value for C_2H_5OH is probably because ethanol has a longer rotational period, despite the similar excited-state lifetimes of ethanol and methanol. It is known that the photoexcited state for methanol at 157 nm has a major character of $n \rightarrow 3p_x(^1A'')$ and that the transition dipole moment is perpendicular to the C−O−H plane. Therefore, it is likely that the corresponding transition dipole of ethanol is also perpendicular to the C−O−H plane. The slightly more negative β value for C_2H_5OH is also probably because the torsional motion of the OH group along the C−O bond for C_2H_5OH is less important than that for CH_3OH.

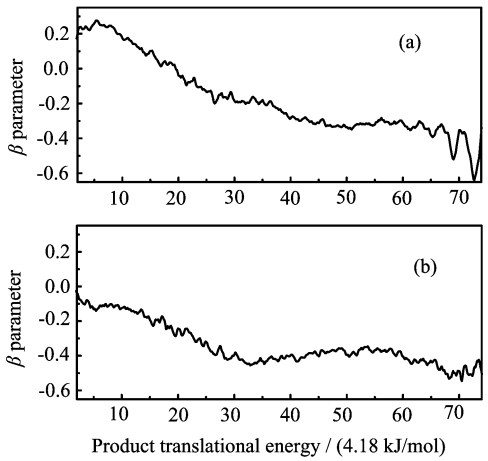

FIG. 7 Anisotropy parameter β as a function of the translational energy for (a) CH_3OH and (b) C_2H_5OH at 157 nm photolysis.

C. Methoxy internal energy distribution

The TOF spectrum in Fig.3(a) has been converted to the total translational energy distribution using a computer program that includes the velocity of the molecular beam. Figure 8 shows the product translational energy distribution for CH_3OH photolysis. The translational energy spectrum between 19000-26000 cm^{-1} with vibrational structures is the main interest in this part. Through the energy conservation, the product translational energy distribution is also the internal energy distribution of the methoxy product. Thus, the structures observed in the product translational energy distribution are all due to the ro-vibrational excited methoxy products.

The spectroscopy of methoxy has been extensively studied both theoretically and experimentally [21-23]. Electronic transition from $\tilde{X}^2E$ to the low-lying excited $\tilde{A}^2A_1$ state for methoxy was studied by using LIF technique, and the recommended vibrational frequencies of

DOI:10.1088/1674-0068/21/04/301-307

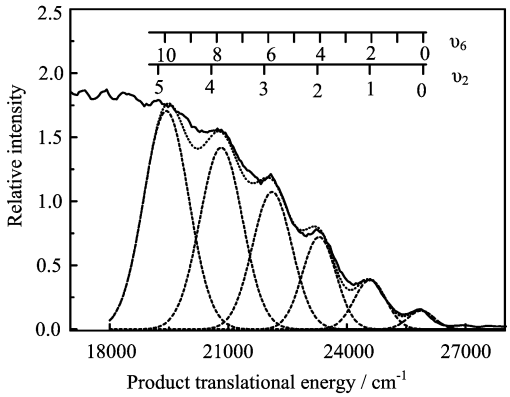

FIG. 8 Translational energy distribution from CH_3OH photodissociation at 157 nm, converted from Fig.3(a). The Gaussian peak fits of the distribution are plotted. The solid line is the experimental spectrum, and the dotted line is the fitted spectrum. The possible vibrational assignments are labeled.

C−H symmetric stretching v_1 , CH_3 umbrella v_2, C−O stretching v_3, C−H asymmetric stretching v_4 , scissors v_5, and CH_3 rocking v_6 are 2943, 1349, 1045, 2774, 1487, and 653 cm^{-1}, respectively [24-26]. Since the regular spacing betwwen the vibrational peaks is around 1250±50 cm^{-1} (see Fig.8), the vibrational structures could be assigned to a progression in the CH_3 rocking ($2v_6$) or CH_3 umbrella (v_2). Of course, the assignment is qualitative and may not be unique. Actually, in one of the simulations, we have included the progressions of the CH_3 rocking and C−O stretching vibrational series, and the simulation is much improved. This suggests that the CH_3O product with C−O stretching excitation is also likely present. This is a little different from that for photolysis of methanol at 193.3 nm, where C−O stretching of methoxy product is prominent [10]. It is obvious that the vibrational state distribution shown in Fig.8 is not statistical, since the population increases as the vibrational energy increases. This is probably because the underlying C−O stretching excitation is very high. This phenomenon also indicates that photodissociation of methanol on the $3p_x$ surface has complicated dissociation mechanism. From the absorption spectrum (Fig.1) we know that the parent molecule has extensive CH_3 rocking by excitation to the $3p_x$ surface. Thus, the CH_3 rocking or CH_3 umbrella excitation in the methoxy radical observed in our experiments likely comes from vibrational excitation of the parent molecule. This is interesting that the vibrational excitation is conserved in the dissociation process.

The vibrational state distribution for C_2H_5OH photodissociation is poorly resolved, as shown in Fig.3(b). This is probably because more vibrational modes of C_2H_5O are excited, such as v_7 (CH_2 wag, 1370 cm^{-1}), v_9 (C−O stretching or C−C−O symmetric stretching, 1067 cm^{-1}), v_{10} (C−C stretching or C−C−O asymmetric stretching, 875 cm^{-1}), and v_{11} (C−C−O bending, 442 cm^{-1}). It is similar to that for 193.3 nm photolysis of ethanol, where C−C stretch and C−C−O bending of ethoxy were involved [16].

IV. DISCUSSION

It is clear that the dissociation of methanol on the $3p_x$ Rydberg surface is significantly more complicated than dissociation on the 3s surface. While the dynamics on the 3s Rydberg electronic state has been successfully elucidated, few studies of the dynamics on the $3p_x$ electronic surface have been reported. An *ab initio* calculation [7] shows that there is an avoided crossing between the 3s and $3p_x$ surfaces, suggesting that there are strong coupling between the two surfaces. Considering the fact that both the C−O bond and the O−H bond are repulsive on the 3s surface, it seems clear that the system undergoes fast internal conversion to the 3s surface after it is excited to the 3p state, and then dissociates on the 3s surface. This is quite reasonable since the observed TOF peak (Fig.3(a)), which corresponds to hydroxyl H loss process, is fast and quite sharp. Another interesting experimental result is the vibrational structures observed in the translational energy spectrum shown in Fig.8. Theoretical studies [7,27] show that the dissociation trajectory on the 3s surface reflects almost exclusively into the O−H dissociation valley due to the barrier on the C−O dissociation channel. The C−O bond is elongated on the 3s surface and vibrates around its equilibrium length in methoxy, and this vibrational motion is carried into the methoxy product during the prompt departure of the H atom along the O−H dissociation pathway. This is the reason that extensive C−O stretch of methoxy is prominent for photodissociation of methanol at 193.3 nm. However, this is not true for photodissociation of methanol at 157 nm, where CH_3 rocking or CH_3 umbrella of methoxy is prominent. This is likely due to the large CH_3 rocking excitation in the methanol at 157 nm. The anisotropy parameter changes dramatically as a function of the product translational energy, also indicating that surface coupling plays an important role. The negative anisotropy parameter in the high translational energy region indicates that the transition dipole moment is nearly perpendicular to the C−O−H plane. Compared to the previous experimental results, the angular anisotropy of H atoms for photolysis at 157 nm is smaller than that at 193 nm, where the β value was determined to be −0.7. This is due to the torsional motion of the OH group along the C−O bond on the 3p surface.

Photodissociation dynamics of ethanol at 157 nm is similar to that of methanol. Considering the fact that the localized electronic transitions involved are essentially the same for both species, it is conceivable that the C−O and O−H dependent part of the 3s and 3p surfaces of methanol and ethanol are similar. Thus, The large product translational energy release P(E)(1′) in

DOI:10.1088/1674-0068/21/04/301-307

Fig.5(b) and the similarly negative anisotropy parameter of ethanol indicate a fast internal conversion from 3p to 3s surface followed dissociation on the repulsive part of the 3s surface along the O−H coordinate. However, subtle yet striking differences between ethanol and methanol are also observed due to the additional CH_3 group. From the TOF spectrum of ethanol shown in Fig.3(b), no vibrational structures are observed. This is probably because severe overlapping of the vibrational manifolds for different vibrational modes. This phenomenon is also observed in the photodissociation of ethanol at 193 nm, where C−C−O motion (C−O stretch, C−C stretch, and C−C−O bending) is excited. The slightly more negative β value for ethanol indicates ethanol has a longer rotational period. The negative β value also indicates the electronic transition dipole moment is perpendicular to the C−O−H plane.

V. CONCLUSION

The 157 nm photodissociation of methanol and ethanol has been investigated using HRTOF technique. Simulation of the H-atom TOF spectra reveals three different atomic H loss processes: one type of direct hydroxyl H elimination and two types of methyl (ethyl) H elimination. Experimental results indicate that the secondary dissociation of the ethoxy radical is less important than that of the methanol radical. The H-atom product angular distribution of methanol is slightly anisotropic (with $\beta\approx-0.3$), indicating the transition dipole moment is perpendicular to the C−O−H plane. The slightly more negative β value for ethanol implies that ethanol has a longer rotational period. The high translational energy release and negative anisotropy parameter suggest that the hydroxyl H undergoes fast conversion from the $3p_x$ surface to the repulsive 3s surface. Furthermore, the translational energy release spectrum from methanol exhibits progressions of 1250 ± 50 cm^{-1}, which are attributed to excitation in the CH_3 rocking or CH_3 umbrella of the methoxy product. The vibrational state distribution is obviously not statistical. An unambiguous interpretation for this awaits detailed theoretical analysis.

VI. ACKNOWLEDGMENTS

This work was supported by Chinese Academy of Sciences via the grant of the CAS international collaboration group, the Ministry of Science, and Technology of China and the National Natural Science Foundation of China.

[1] M. B. Robin, *Higher Excited States of Polyatomic Molecules,* Academic Orlando: FL, 245 (1985); and references therein.
[2] J. G. Galvert and J. N. Pitts, *Photochemistry,* New York: Wiley, 441 (1966).
[3] J. B. Nee, M. Suto, and L. C. Lee, Chem. Phys. **98**, 147 (1985).
[4] E. Sominska and A. Gedanken, J. Mol. Spectrosc. **175**, 234 (1996).
[5] R. Schmiedl, U. Meier, and K. H. Welge, Chem. Phys. Lett. **81**, 495 (1981).
[6] S. Satyapal, J. Park, R. Bersohn, and B. Katz, J. Chem. Phys. **91**, 6873 (1989).
[7] R. J. Buenker, G. Olbrich, H. P. Schuchmann, B. L. Schurmann, and C. von Sonntag, J. Am. Chem. Soc. **106**, 4362 (1984).
[8] E. Kassab, J. T. Gleghorn, and E. M. Evleth, J. Am. Chem. Soc. **105**, 1746 (1983).
[9] C. C. Marston, K. Weide, R. Schinke, and H. U. Suter, J. Chem. Phys. **98**, 4718 (1993).
[10] Y. Wen, J. Segall, M. Dulligan, and C. Wittig, J. Chem. Phys. **101**, 5665 (1994).
[11] S. Harich, J. J. Lin, Y. T. Lee, and X. Yang, J. Chem. Phys. **111**, 5 (1999).
[12] S. Harich, J. J. Lin, Y. T. Lee, and X. Yang, J. Phys. Chem. A **103**, 10324 (1999).
[13] B. Cheng, M. Bahou, W. Chen, C. Yui, Y. P. Lee, and L. C. Lee, J. Chem. Phys. **117**, 1633 (2002).
[14] S. H. Lee, H. I. Lee, and Y. T. Lee, J. Chem. Phys. **121**, 11053 (2004).
[15] C. von Sonntag and H. P. Schuchmann, Adv. Photochem. **10**, 59 (1977); and references therein.
[16] K. H. Xu, G. Amaral, and J. S. Zhang, J. Chem. Phys. **111**, 6271 (1999).
[17] L. Schneider, W. Meier, K. H. Welge, M. N. R. Ashfold, and C. Western, J. Chem. Phys. **92**, 7027 (1990).
[18] L. Schnieder, K. Seekamp-Rahn, E. Wrede, and K. H. Welge, J. Chem. Phys. **107**, 6175 (1997).
[19] C. Sosa and H. B. Schlegel, J. Am. Chem. Soc. **109**, 7007 (1987).
[20] R. N. Zare, Mol. Photochem. **4**, 1 (1972).
[21] S. C. Foster and T. A. Miller, J. Phys. Chem. **93**, 5986 (1989).
[22] S. C. Foster, Y. Hsu, C. P. Damo, X. Liu, C. Kung, and T. A. Miller, J. Phys. Chem. **90**, 6766 (1986).
[23] X. Q. Tan, J. M. Williamson, S. C. Foster, and T. A. Miller, J. Phys. Chem. **97**, 9311 (1993).
[24] T. Ebata, H. Yangishita, K. Obi, and I. Tanaka, Chem. Phys. **69**, 27 (1982).
[25] S. D. Brossard, P. G. Carrick, E. L. Chappell, S. L. Hulegaard, and P. C. Engelking, J. Chem. Phys. **84**, 2459 (1986).
[26] S. M. Colwell, R. D. Amos, and N. C. Handy, Chem. Phys. Lett. **109**, 524 (1984).
[27] C. Larrieu, A. Dargelos, and M. Chaillet, Nouv. J. Chim. **5**, 365 (1981).

DOI:10.1088/1674-0068/21/04/301-307